Variational Image Restoration & Segmentation Models and Approximations

Tony Chan and Luminita Vese

Abstract— **This paper is devoted to some variational problems arising in image recovery and segmentation. We show that classical functionals for image denoising and segmentation like the Mumford-Shah functional and the Total Variation minimization (TV) may be approximated by non-convex functionals and moreover, the edges are better preserved. We also show that our proposed approximations are related to the approximation of Ambrosio-Tortorelli for the Mumford-Shah functional and to an approximation of J. Shah for a TV minimization variant. In these approximations of Ambrosio-Tortorelli and Shah, the functionals depend on two variables (u, v), where u is the image-function and v is an extra variable which allows to detect the contours. Then the problems consist in solving a system with two coupled equations in two unknowns, while in our approximations, the functionals are depending on only one unknown u. We will express v as a function of the gradient of u and this will be our edge-detector. Finally, we compare the models in the framework of image restoration and segmentation. We will see that the obtained results by the new models are better and the algorithms are faster.**

Keywords— **Image restoration and segmentation, variational methods, PDE's, Mumford-Shah functional, Total Variation minimization, non-convex approximations.**

I. Introduction

In the field of image analysis, an important problem is the reconstruction of an original image u, representing a real scene, from an observed and degraded image u_0. The reconstructed image u has to be formed by homogeneous regions, separated by sharp edges. Moreover, the edges must be easily and correctly extracted, as much as possible.

Let us consider u and u_0 as functions defined on a open and bounded domain $\Omega \subset \mathbb{R}^2$, which is in general a rectangle. We assume here that the degradation model is of the form:

$$u_0 = u + \eta,$$

where η represents the noise in the image. We focus on two models proposed to compute u from u_0 using variational methods and regularization are the minimizations of the Mumford-Shah functional ([7]) and of the Total Variation (TV) of u ([8], [9]).

Let us first recall the Mumford-Shah functional for segmentation, in the formulation of L. Ambrosio ([1]):

$$G^{MS}(u) = \int_\Omega \left(\alpha|\nabla u|^2 + \beta|u - u_0|^2\right) dxdy + \mathcal{H}^1(S_u), \tag{1}$$

where α, β are two positive parameters and u_0 is bounded. S_u represents the jumps set of u (the edges) and $\mathcal{H}^1$ is the 1-dimensional Hausdorff measure. This functional has minimizers and moreover, each minimizer is piecewise smooth ([1]).

The second important model is the Total Variation minimization ([8], [9]), where the following functional is minimized:

$$G^{TV}(u) = \int_\Omega \left(\alpha|\nabla u| + \frac{1}{2}|u - u_0|^2\right) dxdy. \tag{2}$$

For these two models, the solution u is a function of bounded variation and only this type of functions allows for discontinuities along edges (the jumps set S_u). For more regular functions, like the Sobolev functions, it is impossible to reconstruct edges.

But, from a numerical point of view, it is not easy to correctly approach functions of bounded variation, due to the jumps on the set S_u of the solution. Especially for the Mumford-Shah functional, the algorithms are complicated, because of the term $\mathcal{H}^1(S_u)$ in the functional (we refer the reader to J. M. Morel, G. Solimini [6], for a review of variational problems and algorithms for image denoising and segmentation).

A solution to this practical problem is proposed by Ambrosio and Tortorelli ([2], [3]): the authors introduce a dual variable v which replaces the jumps set S_u of the solution u, and approach the Mumford-Shah functional by a sequence of functionals depending now on the two variables u and v. We will refer in this

This work is supported in part by ONR Contract N00014-96-1-0277 and NSF Contract DMS-9626755.

Address: UCLA, Mathematics Department, 405, Hilgard Avenue, LOS ANGELES, CA 90095-1555, U.S.A. E-mails: chan@math.ucla.edu, lvese@math.ucla.edu.

paper only to the second approximation of Ambrosio-Tortorelli ([3]), which seems to be simpler than the first ([2]). This approximation for G^{MS} is:

$$G_\rho^{AT}(u,v) = \int_\Omega \Big(\rho|\nabla v|^2 + \alpha v^2|\nabla u|^2 + \frac{(v-1)^2}{4\rho} + \beta|u-u_0|^2\Big), \tag{3}$$

and they showed that if $w_\rho = (u_\rho, v_\rho)$ minimizes G_ρ^{AT}, then (passing to subsequences) u_ρ is an approximation of u, a minimizer of G^{MS}, and v_ρ goes to 1, as $\rho \to 0$, in the $L^2(\Omega)$-topology (i.e. $\int_\Omega |u_\rho - u|^2 \to 0$ and $\int_\Omega |v_\rho - 1|^2 \to 0$, as $\rho \to 0$). Moreover, v_ρ is different from one (and less then one) only in a small neighborhood of S_u, which shrinks as $\rho \to 0^+$.

Following this idea, J. Shah ([10]) proposed an approximation for a Total Variation minimization variant. The approached functional introduced by J. Shah is:

$$\begin{aligned} G^S(u) &= \int_\Omega \Big(\alpha|\nabla u| + \beta|u-u_0|\Big)dxdy \\ &+ \int_{S_u} \frac{\alpha|u^+ - u^-|}{1+\alpha|u^+-u^-|}d\mathcal{H}^1, \end{aligned}$$

where $(u^+ - u^-)$ represents the jump of u across S_u, and the associated approximation is:

$$G_\rho^S(u,v) = \int_\Omega \Big(\rho|\nabla v|^2 + \alpha v^2|\nabla u| + \frac{(v-1)^2}{4\rho} + \beta|u-u_0|\Big). \tag{4}$$

Minimizing these two approximations with respect to u and v yields a system of two coupled equations in two unknowns. We will show in this paper that these models for image restoration and segmentation can be reduced to the minimization of some non-convex functionals depending only on the unknown u, the image-function, and then the problems are reduced to only one equation, making the computation more efficient. Moreover, we will express v as a function of the gradient of u, and in this way we can easily extract the contours of the initially noisy image. From the numerical comparisons, we will see that our algorithms are faster, the obtained results are better and the edges are very-well preserved.

The outline of the paper is as follows. In the next section, we introduce and describe our new approximations, and in Section III we present the numerical results and comparisons. We end the paper by a short concluding section and an appendix, where we give the details of the numerical schemes.

II. The description of the model

The system associated to the minimization of the Ambrosio-Tortorelli approximation $G_\rho^{AT}(u,v)$ from (3) is:

$$\begin{cases} \beta u - \alpha\nabla(v^2\nabla u) = \beta u_0 \\ -\triangle v + \frac{1+4\alpha\rho|\nabla u|^2}{4\rho^2}\Big(v - \frac{1}{1+4\alpha\rho|\nabla u|^2}\Big) = 0. \end{cases} \tag{5}$$

We can see from the second equation of (5) that v is in fact a smoothing of $\frac{1}{1+4\alpha\rho|\nabla u|^2}$.

In this paper we want to reduce this system to only one equation with only one unknown, while still being able to extract the edges.

Our main new idea is to drop the term $-\triangle v$ from the second equation in v of (5) and then v becomes: $v = v_\rho(|\nabla u|) = \frac{1}{1+4\alpha\rho|\nabla u|^2}$. Substituting it in $G_\rho^{AT}(u,v)$ (i.e. without considering the regularizing term $\int_\Omega \rho|\nabla v|^2$ in $G_\rho^{AT}(u,v)$), we obtain, after computation, the functional:

$$G_\rho^{at}(u) = \int_\Omega \Big(\alpha\frac{|\nabla u|^2}{1+4\alpha\rho|\nabla u|^2} + \beta|u-u_0|^2\Big)dxdy.$$

In this way, the following new problem:

$$\begin{cases} \inf_u \Big\{ G_\rho^{at}(u) \Big\} & \text{(restoration for } u\text{)} \\ v_\rho(|\nabla u|) = \frac{1}{1+4\alpha\rho|\nabla u|^2} & \text{(edge-detector)} \end{cases} \tag{6}$$

will be our reduced model for the Ambrosio-Tortorelli approximation (3). Then we no longer have to solve two coupled PDE's, but only one, from the minimization of $G_\rho^{at}(u)$, v being expressed as an explicit function of the gradient $|\nabla u|$ of u.

Similarly, the system associated to the minimization of $G_\rho^S(u,v)$ is:

$$\begin{cases} \beta\frac{u-u_0}{|u-u_0|} - \alpha\nabla\Big(v^2\frac{\nabla u}{|\nabla u|}\Big) = 0, \\ -\triangle v + \frac{1+4\alpha\rho|\nabla u|}{4\rho^2}\Big(v - \frac{1}{1+4\alpha\rho|\nabla u|}\Big) = 0, \end{cases} \tag{7}$$

and again v can be seen to be a smoothing of $\frac{1}{1+4\alpha\rho|\nabla u|}$. Let us drop the term $-\triangle v$ in the second equation of (7). Then we obtain $v = v_\rho(|\nabla u|) = \frac{1}{1+4\alpha\rho|\nabla u|}$ and we substitute it in $G_\rho^S(u,v)$ (i.e. without the regularizing term $\int_\Omega \rho|\nabla v|^2$). We obtain the functional:

$$G_\rho^s(u) = \int_\Omega \Big(\alpha\frac{|\nabla u|}{1+4\alpha\rho|\nabla u|} + \beta|u-u_0|\Big)dxdy.$$

Again, as before, the following new problem:

$$\begin{cases} \inf_u \Big\{ G_\rho^s(u) \Big\} & \text{(restoration for } u\text{)} \\ v_\rho(|\nabla u|) = \frac{1}{1+4\alpha\rho|\nabla u|} & \text{(edge-detector)} \end{cases} \tag{8}$$

will be our reduced model for the Shah approximation, having only one PDE with one unknown u, v being expressed as a function of $|\nabla u|$.

Analogous to these new approximations, we may consider a more general model, as follows: first minimize

$$G_\rho(u) = \int_\Omega \left(\alpha \frac{|\nabla u|^p}{1+4\alpha\rho|\nabla u|^p} + \beta|u-u_0|^p\right) dxdy, \quad (9)$$

with $p \geq 1$, to restore u, and then compute v by:

$$v(|\nabla u|) = \frac{1}{1+4\alpha\rho|\nabla u|^p}$$

as an edge-detector. We obtain from (9) G_ρ^{at} for $p=2$ and G_ρ^s for $p=1$. Finally, in our numerical computations, we use in $G_\rho(u)$ the L^2-norm of $(u-u_0)$ for every $p \geq 1$, instead of the L^p-norm. Then $G_\rho(u)$ becomes (and this will be our new model):

$$G_\rho(u) = \int_\Omega \left(\alpha \frac{|\nabla u|^p}{1+4\alpha\rho|\nabla u|^p} + \beta|u-u_0|^2\right) dxdy. \quad (10)$$

Denoting by ϕ the function

$$z \mapsto \phi(|z|) = \frac{|z|^p}{1+4\alpha\rho|z|^p},$$

we write the Euler equation associated to this minimization problem by

$$\begin{cases} \beta u - \alpha\nabla\cdot\left(\frac{\phi'(|\nabla u|)}{|\nabla u|}\nabla u\right) = \beta u_0, \\ \frac{\partial u}{\partial n}|_{\partial\Omega} = 0. \end{cases} \quad (11)$$

After the computation of the solution u, we compute and present the edge-strength function $v(|\nabla u|) = \frac{1}{1+4\alpha\rho|\nabla u|^p}$.

In order to minimize $G_\rho^S(u,v)$, J. Shah used the associated evolution system ([10]), which is:

$$\begin{cases} \frac{\partial u}{\partial t} + \beta\frac{u-u_0}{|u-u_0|} - \alpha\nabla\cdot\left(v^2\frac{\nabla u}{|\nabla u|}\right) = 0, \\ \frac{\partial v}{\partial t} - \triangle v + \frac{1+4\alpha\rho|\nabla u|}{4\rho^2}v - \frac{1}{4\rho^2} = 0, \\ u(0) = u_0, \quad \frac{\partial u}{\partial n}|_{\partial\Omega} = 0, \quad \frac{\partial v}{\partial n}|_{\partial\Omega} = 0. \end{cases} \quad (12)$$

We will also compare our new model from (11) with the following, which will be called "modified Shah model": in (4) we replace the L^1-norm of $(u-u_0)$ by its L^2-norm. The modified functional obviously is:

$$G_\rho^S(u,v) = \int_\Omega \left(\rho|\nabla v|^2 + \alpha v^2|\nabla u| + \frac{(v-1)^2}{4\rho} + \beta|u-u_0|^2\right), \quad (13)$$

as $\rho \to 0$. Moreover, we use and discretize the associated stationary system to this minimization problem, instead of the evolution system, used by J. Shah:

$$\begin{cases} \beta u - \alpha\nabla\cdot\left(v^2\frac{\nabla u}{|\nabla u|}\right) = \beta u_0, \\ -\triangle v + \frac{1+4\alpha\rho|\nabla u|}{4\rho^2}v - \frac{1}{4\rho^2} = 0, \\ u(0) = u_0, \quad \frac{\partial u}{\partial n}|_{\partial\Omega} = 0, \quad \frac{\partial v}{\partial n}|_{\partial\Omega} = 0. \end{cases} \quad (14)$$

We present in the Appendix the details of the finite differences schemes used for each equation and system.

Remark 1. Let us denote by ϕ_ρ the function:

$$\phi_\rho(t) = \frac{t}{1+4\alpha\rho t}.$$

Then, using these notations, the general model (9) can be written as:

$$G_\rho(u) = \int_\Omega \left(\alpha\phi_\rho(|\nabla u|^p) + \beta|u-u_0|^p\right) dxdy. \quad (15)$$

Note that the function ϕ_ρ is non-convex. For instance for $p=1$, G_ρ^s as $\rho \to 0$ is formally a non-convex approximation of the total variation TV minimization ([8], [9]). Of-course, due to the non-convexity of ϕ_ρ, the problem is, in principle, ill-posed, but the numerical results are very satisfactory, and the algorithms are unconditionally stable.

Remark 2. We will see in the numerical results that $v_\rho(|\nabla u|) = \frac{1}{1+4\alpha\rho|\nabla u|^p}$ may be used as an edge-strength function, and moreover, just like in the theoretical result of Ambrosio-Tortorelli, we will have "numerically" that $v_\rho \to 1$ as $\rho \to 0$, except in a small neighborhood of S_u, which shrinks as $\rho \to 0$.

Remark 3. We can say that our new approximation from (9) with only one variable is a new way of viewing the Ambrosio-Tortorelli approximation and Shah approximation with two variables. Our new model is not equivalent to the approximations of Ambrosio-Tortorelli ($p=2$) and Shah ($p=1$), or even with the Mumford-Shah functional (again $p=2$). We have that $\phi_\rho(|t|^p)$ is a (non-convex) approximation of $|t|^p$. We will see in the numerical results that by minimizing non-convex functionals (as for instance in [12]) in

image recovery, the edges can be better preserved, but unfortunately the problems are often mathematically ill-posed. In this paper, we propose in fact a compromise between the minimization of a convex functional (as for instance the TV minimization, so the problem is well-posed) and the minimization of a non-convex functional (when the edges are better preserved, but the problem is ill-posed): we approach the convex functional by a sequence of non-convex functionals.

III. Numerical results and comparisons

This section is devoted to numerical results and comparisons using the different models described before.

We present in Fig. 1 our synthetic test image (original and noisy), of size 100×100.

Because there is not a rigorous choice of parameters, we use for each model the parameters for which we obtained the best results for the SNR (we can first fix $\beta = 0.5$). We get $\rho = 0.00009$ for each model, but α is different. However, for the models $G^{AT}(u, v)$ and $G^{at}(u)$ we keep the same parameter α, and also for $G^{S}(u, v)$ and $G^{s}(u)$, because the models are in some sense "equivalent", or related. We present each time the reconstructed image u and the edge-strength function v, together with the SNR (the signal to noise ratio) between the original image and the reconstructed image.

We start by presenting in Fig. 2 the best results obtained using the two coupled systems from Ambrosio-Tortorelli (top) and Shah (middle, the evolutionary case) approximations. We see that the reconstructed images are too much regularized and the results for the variable v are still noisy, or contain artificial edges.

Now, by changing the system proposed by J. Shah as described before, the obtained results are better, both for the image u and the edges v, as we may see in Fig. 2 in the bottom (the Modified Shah model). But the edges in v are still not too sharp.

The fact that the edges in the variable v are not sharp using the Ambrosio-Tortorelli and Shah models is due to the isotropic regularizing term $\int_\Omega \rho|\nabla v|^2$ in the functionals, which yields the Laplacian of v (so, a regularization in all directions on v) in each system. In our approach, we do not have an explicit regularizing term on v; our edge-detector $v = v(|\nabla u|)$ is regularized only implicitly, because u is regularized. Using the formulation in two unknowns (u, v) of the problems, to overcome this effect of diffused edges, we can use $\rho\Phi(|\nabla v|)$ as a regularizing term on v in the approximated functionals, where Φ can be a function with at most a linear growth to infinity. For instance, we can consider for Φ the identity, then we obtain $TV(v)$, or a non-convex function. This last possibility has been used in [11], but there is still a coupled system with two equations in two unknowns.

Then we present in Fig. 3 the results obtained with our new model, for different values of p between 1 and 2. We remark that the results are much better than using the modified Shah model, both for the reconstructed images (SNR=22.3 db for the case $p = 1$) and for the edges, represented by the variable v.

We continue the comparisons in Fig. 4, where we presented the same cross-section of v for all models. We classified the results in two groups, the case $p = 1$ in the top, and the case $p = 2$ in the bottom of Fig. 4. This illustrates that the locations of edges are better preserved using the new model, while with the modified Shah model the jumps have been regularized a little bit. We also present the same cross-sections of v in Fig. 5, now in intensity.

In Fig. 6 we compare further the new model with the modified Shah model, representing the SNR function of the time calculation. We remark that the new model is faster, this being obviously due to the fact that the problem was simplified: we solve only one equation and with only one unknown, instead of a coupled-system with two equations and two unknowns. Moreover, we compute $v(|\nabla u|)$ only one time in the end of the algorithm, while in the both Shah model and modified Shah model, is necessary to compute in parallel u and v, at each iteration.

Finally, in Fig. 7 we present the results using the new model u, $v(|\nabla u|)$, and the cross-section of $v(|\nabla u|)$ for $y = 73$ (Fig. 8), for a decreasing sequence of ρ to 0, in the case $p = 1$, in order to illustrate the behavior of the solution as a function of ρ. We remark that the parameter ρ has a regularizing effect on the solution u, but forces $v_\rho(|\nabla u|)$ to be different from 1 only on the set S_u, which shrinks as $\rho \to 0$.

Note that we use the same value of ρ in all cases. The model in the case $p = 2$ regularizes better the edge-strength function $v(|\nabla u|)$ in the homogeneous regions, and the edges in v are darker than in the case $p = 1$ (the values on S_u of v are closer to 0 than in the case $p = 1$). Even though in the result from Fig. 3 the case $p = 1$, the edges in v are not so dark, we can overcome this by doing a thresholding on v. However, in the cases $p = 1$ and $p = 1.25$, we consider that the edges have been extracted the best, because there is no noise on the contours, like in the cases $p = 1.75$ and $p = 2$.

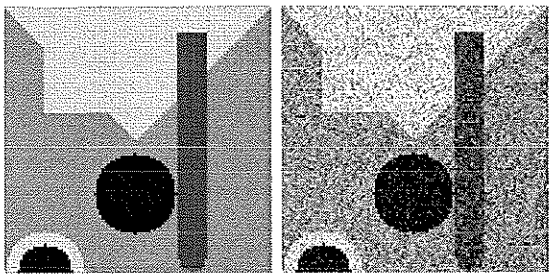

Fig. 1. The original image and the noisy image u_0 (SNR=7.38 db).

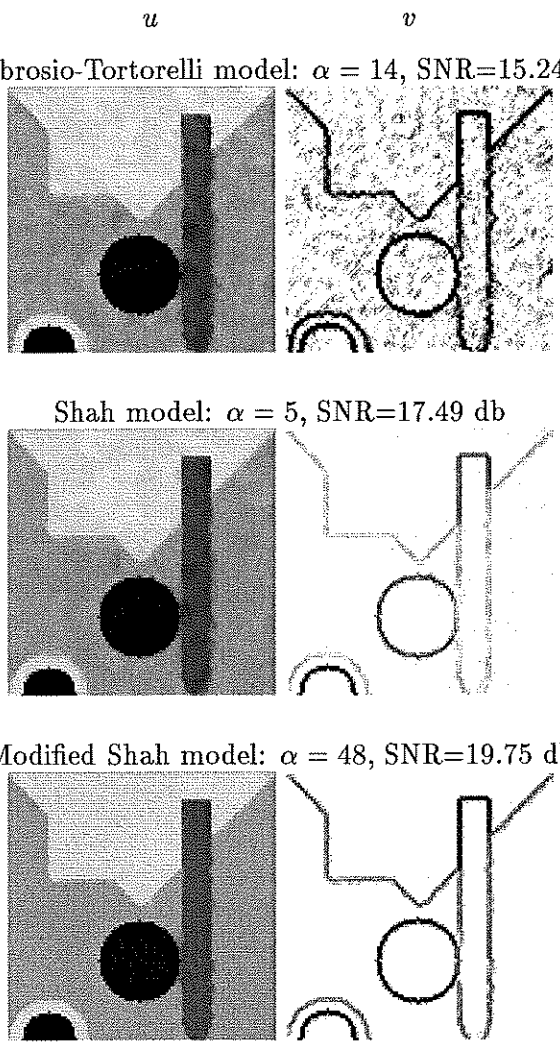

Fig. 2. From left to right, top to bottom: results (u, v) obtained using Ambrosio-Tortorelli, Shah and modified Shah approximations.

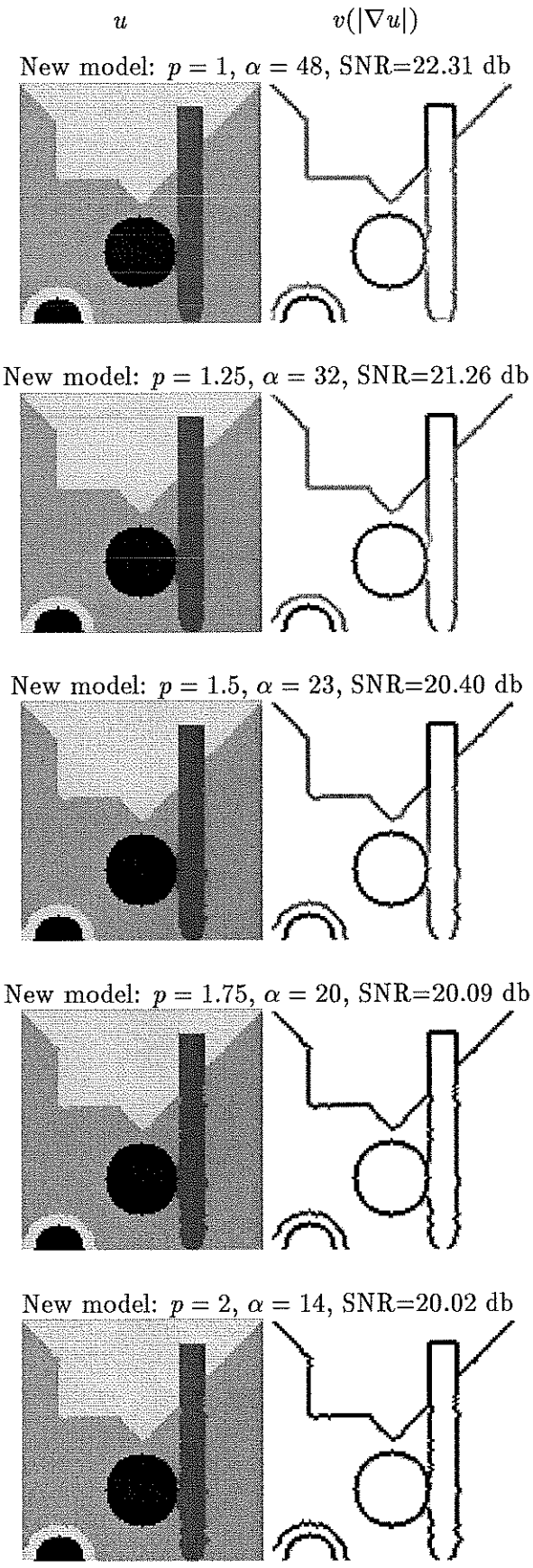

Fig. 3. From left to right, top to bottom: results using the new model u, $v(|\nabla u|)$, for $p = 1,\ 1.25,\ 1.5,\ 1.75,\ 2$.

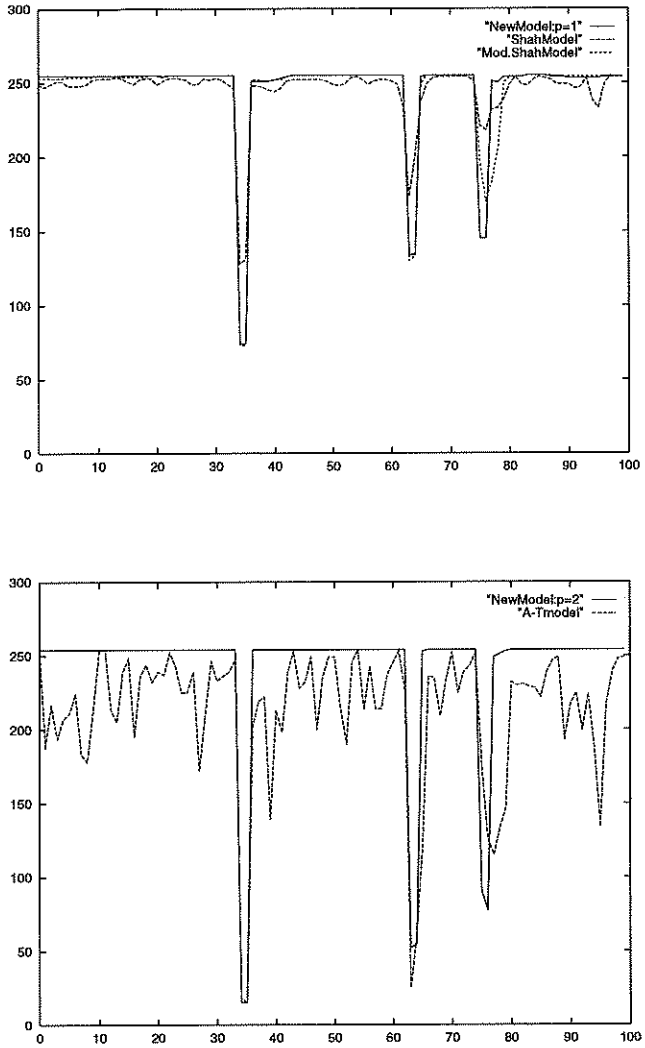

Fig. 4. Cross-sections for $y = 73$ of the edge-strength function v. Top: for the new model $p = 1$, Shah model and Modified Shah model. Bottom: for the new model $p = 2$ and Ambrosio-Tortorelli model.

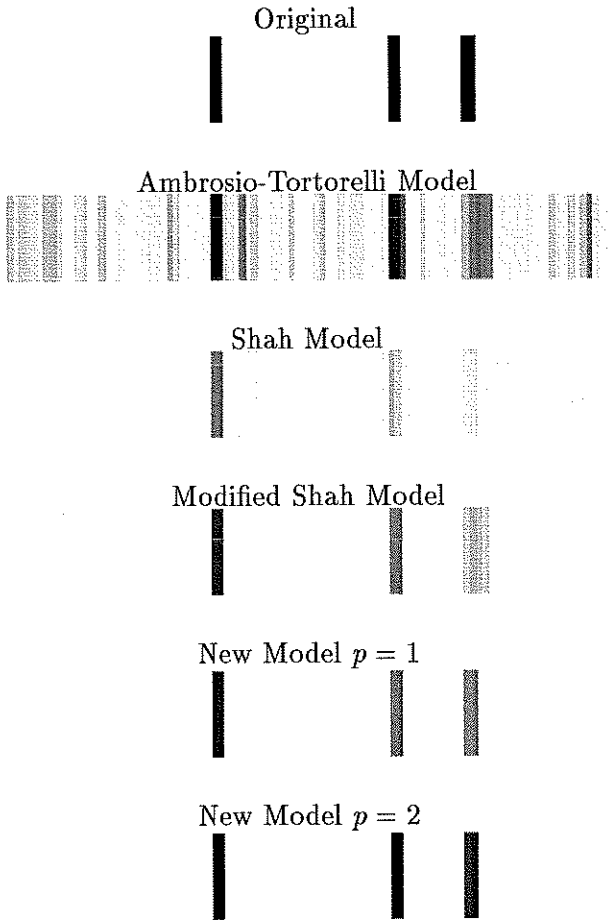

Fig. 5. The lines $y = 73$ in intensity for v. From top to bottom: the original image and the results: Ambrosio-Tortorelli, Shah, Modified Shah approximations, New Model $p = 1$ and New Model $p = 2$.

SNR

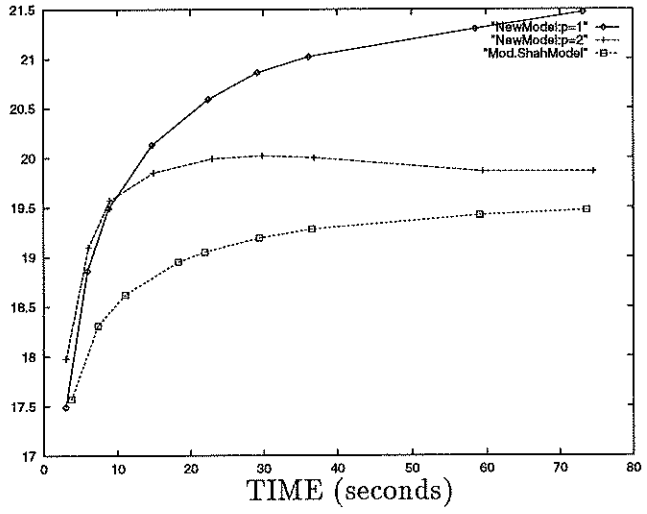

Fig. 6. SNR function of the time calculation, for the new model ($p = 1$ and $p = 2$) and modified Shah model.

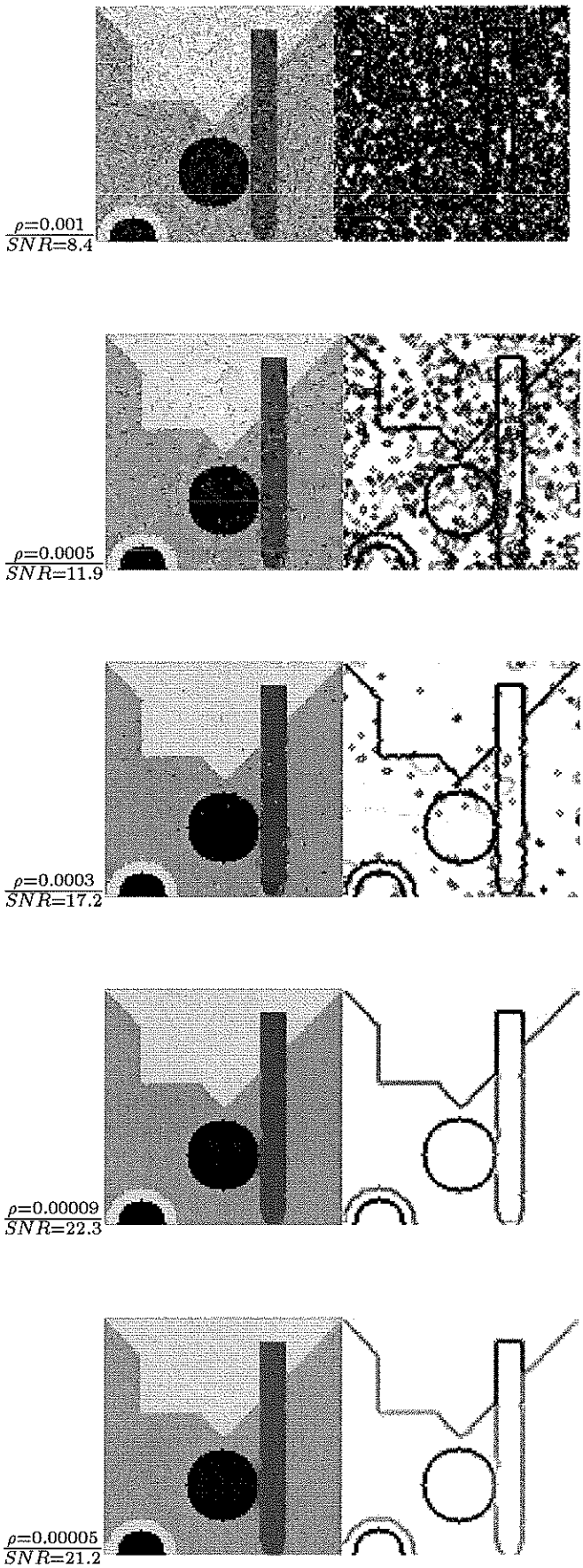

Fig. 7. The behavior of the results for the new model $p = 1$, as $\rho \to 0$. From left to right: u, $v_\rho(|\nabla u|)$.

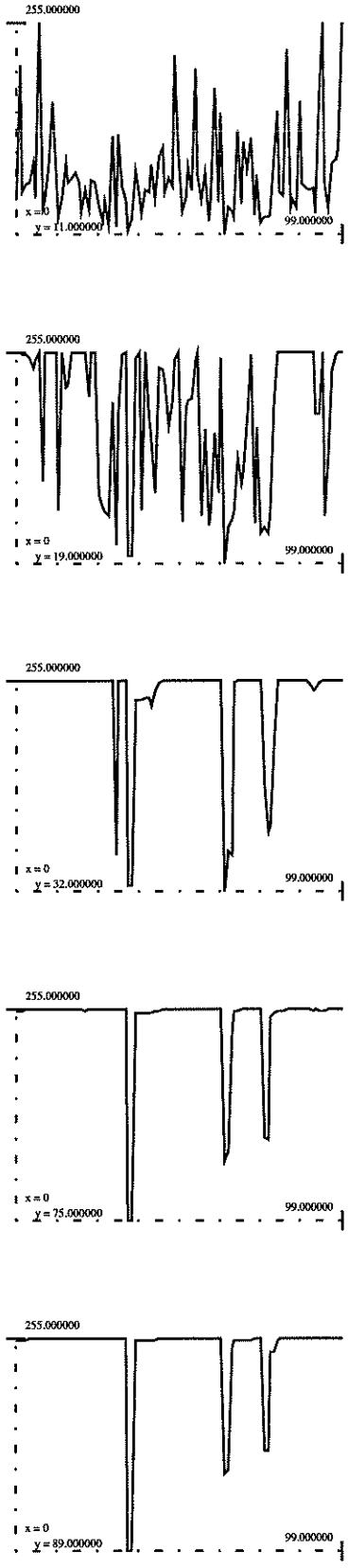

Fig. 8. The associated cross-sections of $v_\rho(|\nabla u|)$ for $y = 73$, from Fig. 7.

IV. Conclusion

In this paper, we have introduced some non-convex approximations, related to an approximation of Ambrosio-Tortorelli for the Mumford-Shah functional, and to an approximation of J. Shah for a variant of the Total Variation minimization. We reduced and simplify their approximations with two coupled equations in two unknowns, to approximations by only one equation in only one unknown, while being able simultaneously to denoise and extract the edges. We deduced a general class of approximations. Finally, by the numerical comparisons, we illustrated that, at least for piecewise-constant images, the results are better and faster, and the edges are very-well preserved. This methods can be applied, for instance, to medical imaging, where the images are generally piecewise-constant.

Appendix

In this section we will describe the finite differences schemes and the fixed point algorithms used in the discretization of the models.

For the equation (11), we use for instance a finite differences implicit scheme based on the method of Rudin-Osher-Fatemi ([9]) to discretize the divergence operator and an iterative (or fixed point) algorithm ([4], [12], [13]). The resulting scheme is unconditionally stable, even if the functional that we minimize is non-convex (see [4], [12]). We note that there are others possible schemes, like the primal-dual method of T. Chan, G. Golub and P. Mulet ([5]).

The algorithm used here is the following: given $u^0 = u_0$, compute u^{n+1} from the linear problem:

$$u^{n+1} - \alpha\nabla\cdot\Big(\frac{\phi'(|\nabla u^n|)}{|\nabla u^n|}\nabla u^{n+1}\Big) = u_0,$$

using Neumann boundary conditions. The details of the scheme can be found in [4] and [12].

To solve numerically the system (12), we use a finite differences scheme of the same type, applied to the following linearization: given $u^0 = u(0) = u_0$, and $v^0 = v_0$, we compute u^{n+1} and v^{n+1} by:

$$\begin{cases} \frac{u^{n+1}-u^n}{\triangle t} + \frac{u^{n+1}-u_0}{2|u^n-u_0|} - \alpha\nabla\cdot\Big((v^n)^2\frac{\nabla u^{n+1}}{|\nabla u^n|}\Big) = 0, \\ \frac{v^{n+1}-v^n}{\triangle t} - \triangle v^{n+1} + \frac{1+4\alpha\rho|\nabla u^n|}{4\rho^2}v^{n+1} - \frac{1}{4\rho^2} = 0, \end{cases} \tag{16}$$

using Neumann boundary conditions. Here, we initialize v_0 by $v_0 = v_\rho(|\nabla u_0|) = \frac{1}{1+4\alpha\rho|\nabla u_0|}$.

The linearization of the system (14) will be, as before:

$$\begin{cases} u^{n+1} - \alpha\nabla\cdot\Big((v^n)^2\frac{\nabla u^{n+1}}{|\nabla u^n|}\Big) = u_0, \\ -\triangle v^{n+1} + \frac{1+4\alpha\rho|\nabla u^n|}{4\rho^2}v^{n+1} - \frac{1}{4\rho^2} = 0, \\ u^0 = u_0, \quad v^0 = v_0 = v_{u_0} = \frac{1}{1+4\alpha\rho|\nabla u_0|}. \end{cases} \tag{17}$$

In order to give an idea about the numerical schemes, we mention only the following: to see how we discretize the divergence operators from each equation, let us consider a general divergence operator of the form:

$$\frac{\partial}{\partial x}\Big(\psi(x,y,u_x,u_y)u_x\Big).$$

We use the following discretization:

$$\frac{1}{h}\triangle_-^x\Big[\Big(\psi\Big(x_i,y_j,\Big(\frac{\triangle_+^x u_{ij}}{h}\Big),\frac{u_{ij+1}-u_{ij-1}}{h}\Big)\Big)\Big(\frac{\triangle_+^x u_{ij}}{h}\Big)\Big]$$

where $\triangle_+^x u_{ij} = u_{i+1j} - u_{ij}$, $\triangle_-^x u_{ij} = u_{ij} - u_{i-1j}$, h being the step space. We also use:

$$\triangle v_{ij} = \frac{1}{h^2}(v_{i+1,j} + v_{i-1,j} + v_{i,j+1} + v_{i,j-1} - 4v_{ij}).$$

The same method is used in the discretization of the system (5), obtained from the Ambrosio-Tortorelli approximation.

References

[1] L. Ambrosio, "A compactness theorem for a special class of functions of bounded variation", *Boll. Un. Mat. Ital.* (7), 3-B (1989), pp. 857-881.

[2] L. Ambrosio and V. Tortorelli, "Approximation of Functionals Depending on Jumps by Elliptic Functionals via $\Gamma-$Convergence", *Comm. on Pure and Applied Mathematics*, Vol. XLIII(1990), pp. 999-1036.

[3] L. Ambrosio and V. Tortorelli, "On the Approximation of Free Discontinuity Problems", *Bollettino U.M.I.* (7) 6-B (1992), 105-123.

[4] G. Aubert and L. Vese, "A variational method in image recovery", *SIAM J. Numer. Analysis*, Vol. 34, No. 5, pp. 1948-1979, October 1997.

[5] T. Chan, G. Golub and P. Mulet, "A nonlinear primal-dual method for Total Variation-based image restoration", *U.C.L.A. CAM report*, 95-43, to appear in *SIAM J. Sci. Comp.*

[6] J.-M. Morel and S. Solimini, *Variational Methods in Image Segmentation*, Progress in Nonlinear Differential Equations and Their Applications, Vol. 14, Birkhäuser Boston, 1995.

[7] D. Mumford and J. Shah, "Optimal Approximations by Piecewise Smooth Functions and Associated Variational Problems", *Communications on Pure and Applied Mathematics*, Vol. XLVII(1989), pp. 577-685.

[8] L. Rudin, S. Osher, "Total variation based image restoration with free local constraints", *Proc. 1st IEEE ICIP*, 1994, Vol. 1, pp. 31-35.

[9] L. Rudin, S. Osher, E. Fatemi, "Nonlinear total variation based noise removal algorithms", *Physica D*, 60(1992), pp. 259-268.

[10] J. Shah, "A Common Framework for Curve Evolution, Segmentation and Anisotropic Diffusion", *Proceedings of I.E.E.E. Conference on Computer vision and pattern recognition*, San Francisco, June 18-20, 1996, pp. 136-142.

[11] S. Teboul, L. Blanc-Féraud, G. Aubert and M. Barlaud, "Variational Approach for Edge-Preserving Regularization using Coupled PDE's", submitted to *IEEE Trans. on Image Processing*.

[12] L. Vese, *Variational problems and PDE's for image analysis and curve evolution*, P.H.D. Thesis, University of Nice, Nov. 1996.

[13] C. R. Vogel and M. E. Oman, "Iterative methods for total variation denoising", *SIAM J. Sci. Statist. Comput.*, 17(1996), pp. 227-238.